

# Soft core thermodynamics from self-consistent hard core fluids

Elisabeth Schöll-Paschinger<sup>1</sup> and Albert Reiner<sup>2</sup>

<sup>1</sup>*Fakultät für Physik, Universität Wien,  
Boltzmannngasse 5, A-1090 Wien, Austria*

<sup>2</sup>*Teoretisk fysikk, Institutt for fysikk,  
Norges teknisk-naturvitenskapelige universitet (NTNU) Trondheim,  
Høgskoleringen 5, N-7491 Trondheim, Norway*

(Dated: September 14, 2018)

## Abstract

In an effort to generalize the self-consistent Ornstein-Zernike approximation (SCOZA) – an accurate liquid-state theory that has been restricted so far to hard-core systems – to arbitrary soft-core systems we study a combination of SCOZA with a recently developed perturbation theory. The latter was constructed by Ben-Amotz and Stell [J. Phys. Chem. B 108,6877-6882 (2004)] as a reformulation of the Week-Chandler-Andersen perturbation theory directly in terms of an arbitrary hard-sphere reference system. We investigate the accuracy of the combined approach for the Lennard-Jones fluid by comparison with simulation data and pure perturbation theory predictions and determine the dependence of the thermodynamic properties and the phase behavior on the choice of the effective hard-core diameter of the reference system.

## I. INTRODUCTION

In its most general formulation, the Self-Consistent Ornstein-Zernike Approximation (SCOZA, [1, 2, 3]) can be obtained from a chosen liquid state theory by the introduction of an adjustable parameter (such as an effective temperature) and the subsequent imposition of consistency between two different routes to thermodynamics, typically the energy and compressibility routes. Simple as this prescription is, it has nevertheless proved to be highly effective and to lead to very accurate predictions for structure and thermodynamics throughout the temperature-density plane, and for the critical point and phase coexistence in particular [4, 5, 6, 7]. Indeed, SCOZA is one of only very few liquid state theories that do not develop serious problems in the critical region and even exhibit some form of scaling with non-classical, partly Ising-like critical exponents [8].

While this is by no means inherent to the concept of SCOZA, applications to continuum fluids have been restricted in a number of ways for both historical and practical reasons: Originally the theory grew out of the semi-analytic solution of the Mean Spherical Approximation (MSA) for hard core Yukawa potentials. Correspondingly, SCOZA has so far only been used with an MSA-like closure and with potentials composed of a hard core of diameter  $\sigma_H$  and an attractive tail  $v_A(r)$ , a situation we will refer to as the “hard-attractive” (HA) one. As far as  $v_A$  is concerned, the original restriction to a single Yukawa term [6] has gradually been relaxed, first by expanding the class of admissible tails to superpositions of two [9] or more Yukawa terms [10],

$$v_A(r) = \sum_{\nu} \epsilon_{\nu} \frac{\sigma_H}{r} e^{-z_{\nu}(r-\sigma_H)},$$

and then to those of Sogami-Ise form [11],

$$v_A(r) = \sum_{\nu} \left( \epsilon_{\nu}^{(1)} \frac{\sigma_H}{r} + \epsilon_{\nu}^{(2)} \right) e^{-z_{\nu}(r-\sigma_H)},$$

for which semi-analytic results are also available, only to be fully overcome through the introduction of a fully numerical solution of the Ornstein-Zernike (OZ) equation [12]. Approximation of  $v_A(r)$  as the superposition of a rather small number of Yukawa or Sogami-Ise tails — a non-trivial step for some of the artificial model potentials used in liquid state theory such as, *e. g.*, the square well one — is thus no longer necessary, and it becomes possible to use exactly the same interaction as the simulations one may want to compare with. Not surprisingly, the flexibility so gained comes at substantial computational cost in solving the SCOZA partial differential equation (PDE).

Despite this liberation of the form of the attractive tail, application of SCOZA has so far remained tied to a hard core reference fluid (marked by subscript H) with potential

$$v_H(r) = \begin{cases} +\infty & \text{for } r < \sigma_H \\ 0 & \text{for } r > \sigma_H. \end{cases} \quad (1)$$

Only in the case of a bounded interaction like, *e. g.*, the Gaussian one,  $v(r) \propto \exp(-\alpha r^2)$ , has the reference system effectively been eliminated by letting  $\sigma_H$  go to zero formally [13]. But this is not an option for simple liquids where the potential diverges for  $r \rightarrow 0$ , such as the classic Lennard-Jones (LJ) one,

$$v_{LJ}(r) = 4\epsilon \left[ \left( \frac{\sigma}{r} \right)^{12} - \left( \frac{\sigma}{r} \right)^6 \right]. \quad (2)$$

For this or more specific systems the infinitely strong hard core repulsion  $v_H(r)$  present in SCOZA is hardly realistic. It is therefore desirable to generalize the theory to largely arbitrary, strong but soft short-range repulsion  $v_S(r)$  to which a

weak attractive tail  $v_A(r)$  is again added to obtain the full “soft-attractive” (SA) system,

$$v_{SA}(r) \equiv v(r) = v_S(r) + v_A(r). \quad (3)$$

Just as in an approximate SA-SCOZA recently proposed that relies on the virial theorem to gauge the amplitude of the pair distribution function (PDF) at the molecular surface [14], in the present contribution we also opt for the time-honored strategy of representing the soft repulsive core by hard spheres of state-dependent diameter. We therefore need explicit prescriptions for both the state-dependence of this diameter and for any correction terms that may be needed to account for the softness of the reference fluid. In doing so there is considerable latitude, and many different schemes have been proposed and used in the past [15, 16]. For example, the highly successful first order perturbation theory due to Weeks, Chandler and Anderson (WCA, [17]) solves both of these problems by determining  $\sigma_H$  as a function of the temperature  $T = k_B/\beta$  and the particle density  $\rho$  such that the Helmholtz free energies of the soft core reference system and the hard spheres coincide. Determination of the diameter is then rather involved and leads to a dependence not only on temperature but also on density. Even though it has been argued that  $\rho$  dependent  $\sigma_H$  is fundamentally more appropriate [18], the practical advantages of a simple prescription that depends on temperature only often outweighs a slight loss in accuracy. Presumably this accounts for much of the lasting popularity of the Barker-Henderson (BH) theory according to which  $\sigma_H(\beta)$  is computed as [19]

$$\sigma_{BH}(\beta) = \int_0^\infty (1 - e^{-\beta v_S(r)}) dr. \quad (4)$$

In this context a recent first order perturbation theory due to Ben-Amotz and Stell (BAS, [16, 20]) is of particular interest: While WCA consider a general reference system that is in turn mapped onto an effective hard sphere fluid to which

attractions are then added, BAS start from a pure hard sphere reference fluid instead and add two terms to the free energy to account for  $v_S$  and  $v_A$ , respectively. This hard core WCA, or BAS, theory has been shown to yield results of an accuracy comparable to that of the original WCA theory while being insensitive to the precise choice of  $\sigma_H$ . This makes it possible to use an even simpler temperature dependence of the effective diameter  $\sigma_H$  than that of Eq. (4) without loss of accuracy [16], and the resulting scheme combines the advantages of the WCA and BH theories.

It is this BAS approach to the treatment of the reference system that we here set out to combine with SCOZA along the lines of a suggestion first put forward by Raineri and co-workers [20]. After a short reminder of SCOZA and BAS theory and a presentation of their combination (section II) we apply our BAS SCOZA to the LJ interaction (2), comparing our results with simulation data as well as the predictions of BAS theory (section III). It turns out that we can well reproduce earlier BAS results and, in fact, improve upon them in slightly supercritical isotherms. As far as phase coexistence is concerned, however, the residual diameter dependence of the free energy translates into an uncertainty of the pressure  $P$  and chemical potential  $\mu$  that renders the coexistence curve more sensitive to variations in  $\sigma_H$  than expected. As shown in the appendix, this is related to the divergence of the compressibility at the critical point. Without a criterion to fix  $\sigma_H(T)$  unambiguously, and in the face of further problems connected to the spinodal of the underlying SCOZA computation if the hard-sphere diameter of the reference system gets too small, the BAS SCOZA considered here is thus found to lack the faculty of predicting the LJ phase diagram with the accuracy one has come to expect from SCOZA. In our concluding remarks we consider the prospects for a SCOZA adapted to non-hard sphere reference systems more generally (section IV).

## II. BAS CORRECTIONS TO SCOZA

The starting point of BAS theory, and hence also of our combined BAS SCOZA, is the splitting (3) of the full potential into its repulsive and attractive components. In the present work we adopt the conventional WCA prescription of separating them at the position  $r_{\min}$  of the potential's minimum, *i. e.*,

$$\begin{aligned} v_S(r) &= \begin{cases} v(r) - v(r_{\min}) & \text{for } r < r_{\min} \\ 0 & \text{otherwise} \end{cases} \\ v_A(r) &= \begin{cases} v(r_{\min}) & \text{for } r < r_{\min} \\ v(r) & \text{otherwise;} \end{cases} \end{aligned} \quad (5)$$

in the LJ case,  $r_{\min} = \sqrt[6]{2}\sigma$  and  $v(r_{\min}) = -\epsilon$ . The Helmholtz free energy of the fluid is customarily written as the sum of the ideal gas contribution  $A^{\text{id}}$  and the excess free energy  $A^{\text{ex}}$ ,

$$A = A^{\text{id}} + A^{\text{ex}}.$$

In computing  $A^{\text{ex}}$ , BAS start from a hard sphere reference system and split  $A^{\text{ex}}$  into the hard sphere term  $A_{\text{H}}^{\text{ex}}$  and two correction terms corresponding to  $v_S$  and  $v_A$ , respectively,

$$A^{\text{ex}} = A_{\text{H}}^{\text{ex}} + \Delta A_S + \Delta A_A.$$

The term  $\Delta A_S$  implementing the difference between hard (H) and soft (S) repulsion is given by [16]

$$\frac{\beta \Delta A_S}{N} = 2\pi\rho \int_0^\infty (g_{\text{H}}(r) - g_{\text{S}}(r)) r^2 dr, \quad (6)$$

where the  $g(r)$  denote the respective PDFs. As in WCA and BAS theories, we relate  $g_S$  to  $g_H$  by the assumption of equal cavity function  $y(r) = g(r) \exp(+\beta v(r))$ . This is expected to be quite harmless for the rather stiff LJ case considered here

[21]. We have checked that the three-term approximation for  $y_H(r)$  inside the core used in Ref. [15] gives essentially the same results as a four-term one due to Grundke and Henderson [22]. Outside the core we adopt Waisman's prescription for the hard sphere structure functions: The direct correlation function  $c_H(r)$ ,  $r > \sigma_H$ , is approximated by a single Yukawa tail with parameters chosen so as to reproduce the Carnahan Starling equation of state through both the compressibility and the virial routes [23], *cf.* appendix A of Ref. [6].

The remaining contributions to the free energy are  $A_H^{\text{ex}}$  and  $\Delta A_A$ . For the former one may use the well-known Carnahan-Starling result [24], whereas the latter is given in BAS theory as an integral over  $g_H(r) v_A(r)$  [16]. On the other hand,  $A_{HA}^{\text{ex}} = A_H^{\text{ex}} + \Delta A_A$  corresponds to the superposition of hard core repulsion and long-range attraction, *i. e.*, to the potential

$$v_{HA}(r) = v_H(r) + v_A(r).$$

This is precisely the HA situation SCOZA has long been applied to with excellent results. In combining BAS theory and SCOZA it is therefore natural to use SCOZA for the description of this HA sub-problem, and for the computation of  $A_{HA}^{\text{ex}}$  in particular. By adding  $\Delta A_S$  we then arrive at the full excess free energy, from which any remaining thermodynamic quantities may be derived. This recipe was first proposed in Ref. [20].

The first step in computing the thermodynamics of the full SA system along an isotherm at inverse temperature  $\beta$  within the combined BAS SCOZA is the determination of the effective hard sphere diameter  $\sigma_H$ . In view of the purported insensitivity of BAS theory results to the precise choice of  $\sigma_H$ , we generally employ a simple Boltzmann factor criterion (BFC) to fix the temperature dependence of  $\sigma_H$  [16, 20]. According to this criterion, we choose  $\sigma_H(\beta)$  so as to keep  $\beta v_S(\sigma_H)$  constant,  $\exp(-\beta v_S(\sigma_H)) = 1/a_{\text{BFC}}$ . Here we have introduced a parameter  $a_{\text{BFC}}$

whose variation allows us to change  $\sigma_H$  in a consistent way for all temperatures. In Ref. [16], BAS found virtually unchanged results for the parameter range  $2 \leq a_{\text{BFC}} \leq 5$ , which includes the *a priori* preferred value  $a_{\text{BFC}} = e$  [20]. — In some of the computations we also use the BH prescription (4).

With  $\sigma_H$  so determined, the SCOZA part can be handled in the usual way [10] except that the WCA splitting (5) effectively precludes a multi-Yukawa or Sogami-Ise representation of  $v_A(r)$  for  $r > \sigma_H$ . We thus have no choice but to turn to an implementation where the OZ relation, along with the customary SCOZA closure

$$\begin{aligned} g_{\text{HA}}(r) &= 0 & \text{for } r < \sigma_H \\ c_{\text{HA}}(r) &= c_H(r) - K v_A(r) & \text{for } r > \sigma_H, \end{aligned} \quad (7)$$

is solved numerically [12]. The first of the above relations expresses the impenetrability of the effective hard cores whereas the second one describes the effect of the attractive tail on the HA direct correlation function  $c_{\text{HA}}(r)$  outside the core beyond that of hard spheres,  $c_H(r)$ . Comparison immediately shows that this corresponds to the MSA closure with  $\beta$  replaced by a state dependent effective inverse temperature  $K(\beta, \rho)$ . The latter is fixed through the requirement of thermodynamic self-consistency as embodied in the SCOZA PDE

$$\left( \frac{\partial}{\partial \beta} \frac{1}{\chi_{\text{HA}}} \right)_{\rho} = \rho \left( \frac{\partial^2 u_{\text{HA}}}{\partial \rho^2} \right)_{\beta}. \quad (8)$$

Here  $1/\chi_{\text{HA}} = 1 - \rho \int_{\mathbb{R}^3} c_{\text{HA}}(r) d^3r$  so that  $\kappa = \beta \chi_{\text{HA}} / \rho$  is the isothermal compressibility of the HA system as evaluated from the compressibility route, and  $u_{\text{HA}} \equiv U_{\text{HA}}^{\text{ex}} / V = 2\pi\rho^2 \int_{\sigma_H}^{\infty} g_{\text{HA}}(r) v_{\text{HA}}(r) r^2 dr$  is the energy route result for the excess, or configurational, internal energy per unit volume. Solution of this PDE subject to suitable boundary conditions at infinite temperature as well as at vanishing and high density yields both the structural and the thermodynamic properties of the HA system throughout the domain of the PDE. Only below the critical



temperature is there a region of instability or non-convergence that must be excluded from the integration. It is customary to do so through the imposition of an additional boundary at the spinodal so that no SCOZA results are available inside the HA spinodal. For a detailed description of the numerical procedure we refer the reader to the literature [5, 10, 12].

For use in BAS SCOZA, integration of the SCOZA PDE is stopped upon reaching the temperature corresponding to  $\sigma_H$ , and internal energy, free energy, pressure, and chemical potential of the HA system are extracted along this isotherm. Finally, we add the BAS correction terms following from  $\Delta A_S$  in order to arrive at the final SA results for these quantities.

Determination of the SA phase diagram involves repeating this procedure for all the diameters corresponding to the temperature range of interest. As both the HA free energy so obtained and the BAS correction term  $\Delta A_S$  are unique functions of temperature and density, so is their sum  $A^{\text{ex}}$ , the excess free energy of the full SA system. The SCOZA PDE is then trivially fulfilled as long as the thermodynamic quantities are computed by differentiation of  $A^{\text{ex}}$ . On the other hand, the structure of the SA system differs from that of the HA system computed with SCOZA and is therefore not accessible. Consequently, neither the compressibility route nor the energy route to thermodynamics can be evaluated for the SA case within the present approach. In this sense, BAS SCOZA must not be seen as a soft core version of SCOZA but rather as a BAS theory built upon a SCOZA foundation.

### III. APPLICATION TO THE LJ FLUID

In order to gauge the performance of BAS SCOZA as described in the preceding section we now turn to its application to the LJ potential (2) with the WCA splitting (5). For comparison purposes we make use of the molecular dynamics simulation data published by Johnson and co-workers [25] and by Lotfi and co-

workers [26] as well as Monte Carlo (MC) results due to Wilding [27]. While the former two directly relate to the full interaction  $v_{\text{LJ}}$  of Eq. (2), the latter are for the cut but not shifted potential  $v_{\text{LJ}}(r)\Theta(2.5\sigma - r)$  without corrections ( $\Theta$  is Heaviside's function). We have therefore exploited the flexibility brought about by the fully numerical solution of the OZ relation and performed BAS SCOZA computations with both of these potentials, depending on the simulation data we want to compare with.

In presenting their theory [16, 20] as well as in their comparative study of various thermodynamic perturbation theories [15], BAS focussed on high densities, and mostly on rather high temperatures: With only a single subcritical temperature and with densities that are at least twice the critical one, all of the four states repeatedly considered in Ref. [16] are quite far from the critical point and the spinodal. Presumably they were chosen because it is in dense or hot systems that particles explore distances around  $\sigma_{\text{H}}$  effectively so that high temperatures and densities present the most challenging test for a perturbative description of soft cores. The effects of variations of  $\sigma_{\text{H}}$  generally increase with density for the isotherms studied in Ref. [16] as well as in our own calculations.

For a comparison of BAS SCOZA with pure BAS theory (or actually,  $\Delta A_{\text{S}}$  being identical in both cases, of their HA parts only) these states are only of limited interest: At high density, the pair structure is dominated by packing effects so that any difference between  $\beta$  and the parameter  $K$  of the closure (7) hardly affects the HA energy integral and the free energy obtained from it by thermodynamic integration. For the lower density states, on the other hand, the high temperatures and great separations from the critical region imply that the SCOZA self-consistency problem can hardly have changed  $K/\beta$  from unity appreciably and so again render the HA structure and thermodynamics of BAS SCOZA equivalent to pure BAS theory. Any remaining discrepancies in the thermodynamics must be attributed to the difference between first-order perturbation theory and what is essentially

the MSA for the HA problem. It is therefore no surprise that BAS SCOZA reproduces the BAS results for these states very well. A detailed comparison of the data underlying Fig. 1 with the corresponding Fig. 2 of Ref. [16] does, however, seem to hint at a sensitivity of  $A^{\text{ex}}$  to variation of  $\sigma_{\text{H}}$  that is slightly reduced *vis-à-vis* BAS theory at  $T^* \equiv k_B T / \epsilon = 2.81$ ,  $\rho^* \equiv \rho \sigma^3 = 0.85$ , and slightly increased for the smallest  $\sigma_{\text{H}}$  values considered at  $T^* = 0.75$ ,  $\rho^* = 0.84$ ; for the latter temperature, however,  $\sigma_{\text{H}} \sim 0.94$  corresponds to  $a_{\text{BFC}} \sim 10^2$ , which is far outside the normal range,  $2 \leq a_{\text{BFC}} \leq 5$ . For the two remaining states,  $T^* = 3.05$ ,  $\rho^* = 1.1$  and  $T^* = 1.35$ ,  $\rho^* = 0.65$ , any differences are too small to be made out from Fig. 2 of Ref. [16].

SCOZA differs from MSA mainly in the critical region and in the vicinity of the spinodal where  $K$  strongly deviates from  $\beta$ . In order to see a genuine SCOZA contribution, as opposed to merely gauging the accuracy of a first order perturbation theory for the HA subproblem, our interest is naturally drawn closer to the HA critical point, and thus also closer to the critical point of the full SA system. Of the isotherms displayed in Fig. 4 of Ref. [16], the one at  $T^* = 1.35$  should already be sufficiently close to the critical temperature of the full LJ interaction that has been estimated as  $T_c^* = 1.310$  [26] and 1.313 [25] by molecular dynamics, and  $T_c^* = 1.3120(7)$  [28] and 1.326(2) [29] by Monte Carlo methods. Unfortunately, BAS only show  $Z = \beta P / \rho$  in the figure so that it is difficult to discern whether a van der Waals loop is present, nor do they address this question directly. On the other hand, the standard by which the performance of BAS theory is judged in Ref. [16] is the classic WCA theory. As all of BH theory, WCA theory, and a thermodynamically self-consistent variant of the latter due to Lado display almost identical van der Waals loops at even higher temperature ( $T^* = 1.4$ , *cf.* inset in Fig. 5 of Ref. [15]), we may safely assume that this is true for the BAS result, too. As can be seen from the inset in our corresponding Fig. 2, the same isotherm is correctly predicted to lie above the critical temperature in BAS SCOZA and is in

essentially perfect agreement with the simulation data for  $2.3 \leq a_{\text{BFC}} \leq e$ .

By way of contrast, the same diameters give substantial deviations and show a marked trend towards a van der Waals loop for smaller  $a_{\text{BFC}}$  when BAS SCOZA is replaced by “BAS MSA”, *i. e.*, if  $K$  is restricted to coincide with  $\beta$ , *cf.* inset in Fig. 2. While an adjustment of  $a_{\text{BFC}}$  so as to achieve good agreement with the simulation data in this part of the phase diagram is certainly possible, the resulting diameter may be too small to describe the packing effects at high density correctly. At any rate, for slightly supercritical isotherms like that at  $T^* = 1.4$ , BAS SCOZA not only leads to a better agreement with the pressure data but also proves less sensitive to variations of the diameter. It is therefore superior not only to pure BAS theory (which might be explained by the qualitative difference of perturbation theory *vs.* integral equations) but also to MSA with BAS corrections. The improvements must therefore be attributed to SCOZA’s self-consistency requirement.

Returning to BAS SCOZA, even for this narrow  $a_{\text{BFC}}$  range there appears a systematic, if small, pressure difference that increases with density. Although it is not obvious how to relate the sensitivities to variation of  $\sigma_{\text{H}}$  of different quantities, comparison of Figs. 2 and 3 seems to indicate that the pressure depends on  $\sigma_{\text{H}}$  more strongly than the free energy. A similar conclusion can be drawn for the chemical potential by comparing Figs. 1 and 4. This greater sensitivity of  $P$  and  $\mu$  relative to  $A^{\text{ex}}$  for most states, and for comparatively low temperatures in particular, is also demonstrated in Tab. I where  $\sigma_{\text{H}}$  induced changes are related both to the absolute value and to the density dependence of the respective quantities. It can also be seen in pure BAS theory: For the lowest isotherm in Fig. 4 of Ref. [16],  $T^* = 0.74$ , a slight variation of  $\sigma_{\text{H}}$  from  $\sigma_{\text{BFC}}^{[a=e]}$  by only two per cent is sufficient even to change  $Z$  from a convex to a concave function of density for  $\rho^* \approx 1$ .

Proceeding to the critical region and phase coexistence, in BAS SCOZA the binodal is located as in pure SCOZA *viz.*, by a search for densities of equal pressure

$P$  and chemical potential  $\mu$ ; the critical point is identified with the locus where the gas and liquid branches of the binodal meet. As expected for a variant of BAS theory even if it makes use of SCOZA input, the critical behavior is not compatible with the Ising universality class: In the accessible temperature range the coexistence curve is not described well by the usual scaling form, and for the highest sub-critical temperatures the effective exponent  $\beta$  tends to values far larger than SCOZA's  $7/20$  [8], which in turn slightly exceeds the correct Ising value. This is also conspicuous from the forms of the binodals obtained from the BFC diameter  $\sigma_{\text{BFC}}$  with several values of  $a_{\text{BFC}}$  as well as the BH diameter  $\sigma_{\text{BH}}$  as displayed in Figs. 5 and 6 for the truncated and the full LJ potentials, respectively.

Figs. 5 and 6 also bring out the gravity of the diameter sensitivity of  $P$  and  $\mu$  for the description of phase coexistence: There is a substantial variation in the locations of the upper parts of the coexistence curves when  $\sigma_{\text{H}}$  is changed from  $\sigma_{\text{BFC}}^{[a=2.2]}$  (Fig. 5) or  $\sigma_{\text{BFC}}^{[a=2.3]}$  (Fig. 6). It should be noted that these optimal values of  $a_{\text{BFC}}$  cannot be computed from the theory itself but are merely the results of comparisons with the simulation data for the coexisting densities for the truncated and full potentials, respectively.

The particularly great sensitivity of the binodal at the highest temperatures can in fact easily be understood by linking the shift in the coexisting densities induced by a change in the effective hard core diameter  $\sigma_{\text{H}}$  to the isothermal compressibility  $\kappa$  at phase coexistence. Clearly,  $\kappa$  diverges at the critical point and then decreases along the two branches of the binodal as we proceed to lower temperatures. Informally speaking, a higher compressibility means that the physical system must be compressed or expanded, and therefore its density changed, by a larger amount in order to offset a small change in pressure and chemical potential, which explains the more pronounced effect at higher temperatures. At the same time, the thermodynamic quantities are generally more sensitive to a change in  $\sigma_{\text{H}}$  at higher densities, which explains the asymmetry of the effect between the

low and high density branches of the binodal. A more formal exposition of this reasoning can be found in the appendix.

A different perspective on the strong  $\sigma_H$  dependence of the binodal is offered by the realization that an increase in  $\sigma_H$  renders the HA subproblem more strongly repulsive, thus lowering the HA critical temperature. In an exact theory, the correction term  $\Delta A_S$  strictly compensates this shift of the critical point. From a first-order perturbation theory, however, we can expect only a partial compensation, as is clearly demonstrated in Fig. 7 where we separate the SCOZA and BAS contributions to the free energy. Consequently, a change in  $a_{\text{BFC}}$  (or, more generally, in the prescription for  $\sigma_H(\beta)$ ) still leads to a systematic shift of the SA critical temperature. For any given isotherm, this necessarily corresponds to changes of the coexisting densities that are most pronounced close to the critical point where the binodal gains in width most rapidly.

Such shifts of  $\beta_c$  can actually be inferred from Figs. 5 and 6. The reason they cannot be seen directly is connected to the specific way in which BAS SCOZA combines the theories it is built upon, *viz.*, by adding a BAS correction term to a SCOZA free energy: As mentioned in the introduction, SCOZA suffers from a region where no solution can be found due to either stability or convergence problems. This region is buried within the HA spinodal and is customarily eliminated through the imposition of an artificial spinodal boundary condition. No BAS SCOZA results can therefore be obtained inside the HA spinodal. Depending on the diameter, this hole in the solution may lie well within the SA binodal. For  $a_{\text{BFC}}$  above a certain threshold, however, or more generally whenever  $\sigma_H(\beta_c)$  is too small, the HA interaction is not sufficiently repulsive so that the HA spinodal rises above the SA binodal, the upper part of which is then no longer accessible. As can be seen from Figs. 5 and 6, this is the case for those diameters that come close to the simulated phase diagrams. The hole in the solution for temperatures below the HA critical one can also be seen from the missing intervals in the lowest

temperature isotherms displayed in Figs. 2, 3 and 10.

Let us now consider the configurational internal energy  $U^{\text{ex}} = (\partial\beta A^{\text{ex}}/\partial\beta)_\rho$ . With  $A^{\text{ex}} = A_{\text{HA}}^{\text{ex}} + \Delta A_{\text{S}}$  we obtain  $U^{\text{ex}}$  as the sum of the HA internal energy  $U_{\text{HA}}^{\text{ex}}$  extracted directly from the SCOZA computation with fixed diameter and the correction  $\Delta U_{\text{S}}$  implementing the difference between hard and soft repulsion. The latter is composed of the temperature derivative of the BAS correction  $\Delta A_{\text{S}}$  and a term related to the temperature dependence of  $A_{\text{HA}}^{\text{ex}}$  through  $\sigma_{\text{H}}$  (and thus to the steepness of  $v_{\text{S}}$  at the effective molecular surface),

$$U^{\text{ex}} = U_{\text{HA}}^{\text{ex}} + \Delta U_{\text{S}}$$

$$\Delta U_{\text{S}} = \left( \frac{\partial\beta\Delta A_{\text{S}}}{\partial\beta} \right)_\rho + \left( \frac{\partial\beta A_{\text{HA}}^{\text{ex}}}{\partial\sigma_{\text{H}}} \right)_\beta \frac{d\sigma_{\text{H}}}{d\beta}.$$

Here, the derivative  $d\sigma_{\text{H}}/d\beta$  is to be evaluated according to the convention used to fix  $\sigma_{\text{H}}(\beta)$ , *i. e.*, from Eq. (4) for  $\sigma_{\text{BH}}$ , or at constant  $a_{\text{BFC}}$  for  $\sigma_{\text{BFC}}$ .

From Fig. 8 we see that the overall diameter dependence of the excess internal energy is qualitatively similar to that of the excess free energy, *cf.* Fig. 1. Not surprisingly, it is most pronounced at the highest densities whereas the temperature is of minor importance for the states considered in Fig. 8. This can easily be understood in terms of packing effects that dominate the pair structure. In Fig. 9 we again separate the SCOZA and BAS contributions to the internal energy. Interestingly, the latter compensates the diameter dependence of the former not even approximately as was the case for the free energy (Fig. 7). Instead,  $\Delta U_{\text{S}}$  is essentially constant over the whole  $\sigma_{\text{H}}$  range shown, and the variation of  $U^{\text{ex}}$  is due to  $U_{\text{HA}}^{\text{ex}}$  alone. As Fig. 10 shows, the particularly low sensitivity of  $U^{\text{ex}}$  with respect to  $\sigma_{\text{H}}$  in the upper panel of Fig. 9 is a mere consequence of the transition between density ranges where  $U^{\text{ex}}$  rises or falls, respectively, with growing  $\sigma_{\text{H}}$ . In the lower panel, the internal energy again varies by several per cent in the  $\sigma_{\text{H}}$  range displayed.

Both pressure  $P$  and internal energy  $U^{\text{ex}}$  as computed within BAS SCOZA with  $2.3 \leq a_{\text{BFC}} \leq e$  are generally in good agreement with the simulation results for the sample isotherms displayed in Figs. 2 and 10. Only a detailed comparison reveals some systematic deviations that seem to hint at a moderate state dependence of the optimal value of  $a_{\text{BFC}}$ : At high densities and supercritical temperatures  $U^{\text{ex}}$  is best reproduced with  $a_{\text{BFC}} = e$ , and the simulated pressures indicate an  $a_{\text{BFC}}$  even slightly larger than  $e$ . By way of contrast, phase diagram (Fig. 6), pressure (Fig. 2) and internal energy (Fig. 10) all agree that  $a_{\text{BFC}} = 2.3$  is the optimum value for the full LJ interaction for states for which SCOZA's self-consistency requirement is expected to be relevant, *i. e.*, for  $T < T_c$  as well as for  $T \sim T_c$ ,  $\rho \sim \rho_c$ . A similar level of agreement is also expected for the truncated potential with a slightly larger diameter,  $a_{\text{BFC}} = 2.2$ , *cf.* Fig. 5. This difference of about 0.1 per cent in  $\sigma_{\text{H}}$  seems remarkably small given the pronounced influence on the critical parameters such a cut may have [30], and in particular given the respective critical temperatures  $T_c^* < 1.2$  for the cut potential [27] as opposed to  $T_c^* > 1.3$  for the full interaction [25, 26, 28, 29], *cf.* Figs. 5 and 6.

#### IV. CONCLUSION AND PERSPECTIVES

As we argued at the end of section II, BAS SCOZA should be regarded as a SCOZA-based variant of BAS theory rather than as a modified SCOZA. From this point of view our expectations regarding the performance of this combined theory are well fulfilled: Good agreement with simulation results for binodal, pressure and internal energy can be achieved with a judicious choice of the parameter  $a_{\text{BFC}}$ ; we find a significant improvement over pure BAS theory at slightly supercritical isotherms; and away from the critical region and phase coexistence both schemes give essentially equivalent results. Unfortunately, the transition from pure BAS theory to BAS SCOZA entails a dramatic increase in computational cost as the



solution of a non-linear PDE in  $\beta$  and  $\rho$  is required just for the results along a single isotherm. For the computation of a full phase diagram, BAS SCOZA theory is far more demanding than even fixed-diameter SCOZA where a single integration of the PDE yields the results at all densities and temperatures.

On the other hand, the present scheme was originally proposed as a soft-core extension of SCOZA rather than as an improved BAS theory [20]. And indeed, BAS SCOZA is able to handle SA fluids using the true interaction whereas previous applications of conventional SCOZA to the LJ fluid had to rely on heuristic, and by no means small, corrections to form and amplitude of the potential outside the fixed hard core [9] yielding a critical temperature that is too low by about five per cent [10]. Still, the huge increase in computational cost, the problems connected to the HA spinodal, and the loss of all structural information may seem an inordinate prize to pay for this advantage of BAS SCOZA.

Most importantly, though, the distinctive feature of SCOZA, *viz.*, the thermodynamic consistency requirement implemented by an effective temperature that replaces the true temperature in the MSA closure for the HA system, shows up in the results only in the proximity of the critical point. It is there that we have to look for SCOZA-specific improvements: In the rest of the  $(\beta, \rho)$  plane SCOZA is essentially equivalent to MSA, and any improvements over pure BAS theory merely reflect the superiority of integral equations over perturbation theory in evaluating the difference  $\Delta A_A$  of the free energies of the H and HA systems. Close to the critical point, however, the chief advantage of BAS theory, *viz.*, the near-constancy of the thermodynamic results under variation of  $\sigma_H$  breaks down, and the BAS SCOZA binodal strongly depends on  $\sigma_H(\beta)$ . The value of the parameter  $a_{\text{BFC}}$  thus greatly influences the predicted phase behavior; at the same time, it cannot be computed from the theory itself, and the *a priori* attractive choice of  $a_{\text{BFC}} = e$  [20] is certainly unsatisfactory in the critical region. Further considering that the BAS SCOZA binodals are far from compatible with the Ising universality class

we therefore conclude that the theory as presented here cannot be used to predict the critical properties and liquid-vapor phase behavior from first principles with anywhere near the accuracy usually associated with SCOZA.

As for the feasibility of a BAS-based SCOZA rather than a SCOZA-based BAS theory, the main obstacle to using BAS results to “provide reference-system input” [15] for SCOZA is the purely thermodynamic nature of the BAS term  $\Delta A_S$  that does not allow us to relate the structures of the HA and SA fluids. Without  $K$ -dependent SA structures, however, neither the energy nor the compressibility routes to the SA thermodynamics can be evaluated, and the question of their consistency becomes meaningless. Indeed, inclusion of the soft core contribution in the thermodynamic self-consistency problem is likely to be of prime importance for the performance of an eventual soft core variant of SCOZA [14].

What then, one may ask, are more promising ways towards a SCOZA capable of describing SA systems? For this we see two options: One possibility is to consider formulations where the introduction of an effective hard core reference system still allows the analytical short cuts for the solution of the OZ equation available for the multi-Yukawa or Sogami-Ise fluids to be used and that include the softness in the self-consistency problem, if only approximately; one such approach has recently been proposed [14]. On the other hand, if the hard-won freedom to choose almost arbitrary functions  $v_A$  and  $v_S$  for the attractive and soft-repulsive parts of the interaction is to be retained, the OZ relation must be solved numerically at any rate. In this case there is no need for a hard core reference system, and non-perturbative ways of treating the soft repulsive reference fluid may be more appropriate and less wasteful in terms of computing resources and structural information. We intend to pursue this topic in a further study.

## Acknowledgments

AR wishes to thank Johan Høye for many stimulating discussions and gratefully acknowledges financial support from the Austrian Science Fund (FWF) under project J2380-N08. This work was also supported by the Austrian Science Fund (FWF) under Project No. P17178-N02.

## APPENDIX A: DIAMETER SENSITIVITY OF THE BINODAL

Let us consider a subcritical isotherm,  $\beta > \beta_c$ , with vapor and liquid coexisting at densities  $\rho_v$  and  $\rho_l$ , respectively. Along this isotherm the exact free energy is a function of density only,  $A = A(\rho)$ . The BAS free energy, on the other hand, is computed in an approximate way and makes use of an effective hard sphere reference system with density independent diameter  $\sigma_H$ . It therefore acquires an additional dependence. To obtain the free energy at slightly different values of  $\sigma_H$  and  $\rho$  we can use the first order Taylor expansion

$$A(\rho + \Delta\rho, \sigma_H + \Delta\sigma_H) = A(\rho) + \Delta\sigma_H \dot{A}(\rho) + \Delta\rho A'(\rho) + \dots$$

In this appendix we use dots to denote differentiation with respect to  $\sigma_H$  and primes for differentiation with respect to  $\rho$ . For the benefit of a compact notation we will also use subscripts  $v$  and  $l$  to indicate functions evaluated at  $\rho_v$  and  $\rho_l$ , respectively, as well as subscripts  $+$  or  $-$  for their symmetric and anti-symmetric combinations, *i. e.*,  $\psi_{\pm} \equiv \psi_l \pm \psi_v \equiv \psi(\rho_l) \pm \psi(\rho_v)$  for any quantity  $\psi$ .

By differentiation of the free energy we get analogous relations for the pressure  $P$  and chemical potential  $\mu$ , the two quantities that directly enter the determination of the coexistence curve:

$$P(\rho + \Delta\rho, \sigma_H + \Delta\sigma_H) = P(\rho) + \Delta\sigma_H \dot{P}(\rho) + \Delta\rho P'(\rho) + \dots,$$

$$\mu(\rho + \Delta\rho, \sigma_H + \Delta\sigma_H) = \mu(\rho) + \Delta\sigma_H \dot{\mu}(\rho) + \Delta\sigma_H \mu'(\rho) + \dots$$

For given  $\sigma_H$ , the coexisting densities are obtained from the criterion of equal pressure and chemical potential,  $P(\rho_v, \sigma_H) = P(\rho_l, \sigma_H)$  and  $\mu(\rho_v, \sigma_H) = \mu(\rho_l, \sigma_H)$ . Specializing to the coexisting densities  $\rho_v$  and  $\rho_l$  obtained for this  $\sigma_H$ , the equilibrium conditions reduce to  $P_v = P_l$  and  $\mu_v = \mu_l$ , or

$$P_- = \mu_- = 0. \quad (\text{A1})$$

Non-zero  $\Delta\sigma_H$ , on the other hand, modifies both pressure and chemical potential and is therefore generally accompanied by changes  $\Delta\rho_v$  and  $\Delta\rho_l$  in the coexisting densities. Taking Eq. (A1) into account, switching to symmetric and anti-symmetric combinations of quantities, and simplifying, the equilibrium conditions are easily obtained as

$$P'_- \Delta\rho_+ + P'_+ \Delta\rho_- + 2 \dot{P}_- \Delta\sigma_H = 0,$$

$$\mu'_- \Delta\rho_+ + \mu'_+ \Delta\rho_- + 2 \dot{\mu}_- \Delta\sigma_H = 0$$

to lowest order. Solving for  $\Delta\rho_\pm$  yields the sensitivity of the symmetric and asymmetric shifts in the coexisting densities to a change  $\Delta\sigma_H$  of the effective diameter as

$$\begin{aligned} \frac{\Delta\rho_\pm}{\Delta\sigma_H} &= 2 \frac{P'_\pm \dot{\mu}_- - \mu'_\pm \dot{P}_-}{P'_\mp \mu'_\pm - P'_\pm \mu'_\mp} \\ &= \pm \frac{P'_\pm \dot{\mu}_- - \mu'_\pm \dot{P}_-}{P'_l \mu'_v - P'_v \mu'_l}, \end{aligned}$$

where we have taken advantage of some cancellations in the denominator to arrive at the second expression.

From the product of two density derivatives in the denominator as opposed to single factors of density derivatives in the numerator it is already apparent that the sensitivity of the binodal to variation of  $\sigma_H$  must be proportional to the isothermal

compressibilities  $\kappa_v$  and  $\kappa_l$  at the coexisting densities. To make this more explicit and simplify the expressions further, we introduce the free energy per unit volume  $f$  and use basic thermodynamic relations to replace the pressure and chemical potential, as well as their derivatives, by appropriate expressions in terms of  $f$  and its derivatives while converting reciprocals of  $f''$  to the isothermal compressibilities. After some slightly tedious simplification we get explicit expressions for the shifts in the coexisting densities induced by a change  $\Delta\sigma_H$  of the effective diameter, *viz.*,

$$\begin{aligned}\frac{\Delta\rho_{\pm}}{\Delta\sigma_H} &= \rho_l^2 \kappa_l \left( \dot{f}'_l - \frac{\dot{f}_-}{\Delta\rho_-} \right) \pm \rho_v^2 \kappa_v \left( \dot{f}'_v - \frac{\dot{f}_-}{\Delta\rho_-} \right) \\ &= \frac{\Delta\rho_l}{\Delta\sigma_H} \pm \frac{\Delta\rho_v}{\Delta\sigma_H}.\end{aligned}$$

The change of any one of the coexisting densities with  $\sigma_H$  is thus proportional to the product of the compressibility at that density and a factor that combines the sensitivities of the free energy at both branches of the binodal with its density derivative.

In an exact theory, of course, all the  $\sigma_H$  derivatives vanish exactly and the coexisting densities are strictly independent of  $\sigma_H$  even at the critical point,  $\beta = \beta_c$ ,  $\rho_- = 0$ , where the compressibility diverges. In an approximate theory, on the other hand,  $\dot{f}' - \dot{f}_-/\Delta\rho_-$  is non-zero for  $\beta > \beta_c$ , and while its limit for  $\beta \rightarrow \beta_c$  obviously vanishes, that of its product with the diverging compressibility may be zero, finite, or even infinite; for BAS SCOZA, Figs. 5 and 6 indicate a finite value. As  $\beta$  further increases from  $\beta_c$ , the two branches of the binodal separate rapidly, and the one-sided difference quotient  $\dot{f}_-/\Delta\rho_-$  over the coexistence region no longer cancels the derivative  $\dot{f}'$  at either side of the binodal. The expression in parentheses is therefore no longer expected to be close to zero. In the case of BAS SCOZA, the variability of  $f$  with  $\sigma_H$  strongly increases with density, as is expected for thermodynamic perturbation theories in general. This carries over to  $\dot{f}' - \dot{f}_-/\Delta\rho_-$  and, in combination with the prefactor  $\rho^2$ , so explains why the sensitivity of  $\rho_l$  is

significantly larger than that of  $\rho_v$ .

- 
- [1] J. S. Høye, G. Stell, J. Chem. Phys. **67**, 439 (1977).
  - [2] J. S. Høye, G. Stell, Mol. Phys. **52**, 1071 (1984).
  - [3] J. S. Høye, G. Stell, Int. J. Thermophys. **6**, 561 (1985).
  - [4] R. Dickman, G. Stell, Phys. Rev. Lett. **77**, 996 (1996).
  - [5] D. Pini, G. Stell, R. Dickman, Phys. Rev. E **57**, 2862 (1998).
  - [6] D. Pini, G. Stell, N. B. Wilding, Mol. Phys. **95**, 483 (1998).
  - [7] E. Schöll-Paschinger, D. Levesque, J.-J. Weis, G. Kahl, J. Chem. Phys. **122**, 024507 (2005).
  - [8] J. S. Høye, D. Pini, G. Stell, Physica A **279**, 213 (2000).
  - [9] D. Pini, G. Stell, N. B. Wilding, J. Chem. Phys. **115**, 2702 (2001).
  - [10] E. Schöll-Paschinger, *Phase behavior of simple fluids and their mixtures*, PhD thesis, Technische Universität Wien (2002).
  - [11] E. Schöll-Paschinger, J. Chem. Phys. **120**, 11698(2004).
  - [12] E. Schöll-Paschinger, A. L. Benavides, R. Castañeda-Priego, J. Chem. Phys. **123**, 234513 (2005).
  - [13] B. M. Mladek, G. Kahl, M. Neumann, J. Chem. Phys. **124**, 064503 (2006).
  - [14] J. S. Høye, A. Reiner, accepted for publication in J. Chem. Phys.
  - [15] D. Ben-Amotz, G. Stell, J. Chem. Phys. **119**, 10777 (2003). Erratum: J. Chem. Phys. **120**, 4994 (2004).
  - [16] D. Ben-Amotz, G. Stell, J. Phys. Chem. B **108**, 6877 (2004).
  - [17] J. D. Weeks, D. Chandler, H. C. Andersen, J. Chem. Phys. **54**, 5237 (1971).
  - [18] Y. Tang, J. Chem. Phys. **116**, 6694 (2002).
  - [19] J. A. Barker, D. Henderson, J. Chem. Phys. **47**, 4714 (1967).
  - [20] F. O. Raineri, G. Stell, D. Ben-Amotz, J. Phys.: Condens. Matter **16**, S4887 (2004).
  - [21] D. Ben-Amotz, G. Stell, J. Chem. Phys. **120**, 4844 (2004).

- [22] D. Henderson, E. W. Grundke, J. Chem. Phys. **63**, 601 (1975).
- [23] E. Waisman, Mol. Phys. **32**, 1627 (1973).
- [24] J. P. Hansen, I. R. McDonald, *Theory of simple liquids*, London (Academic) <sup>2</sup>1986.
- [25] J. K. Johnson, J. A. Zollweg, K. E. Gubbins, Mol. Phys. **78**, 591 (1993).
- [26] A. Lotfi, J. Vrabec, J. Fischer, Mol. Phys. **76**, 1319 (1992).
- [27] N. B. Wilding, Phys. Rev. E **52**, 602 (1995).
- [28] J. J. Potoff, A. Z. Panagiotopoulos, J. Chem. Phys. **109**, 10914 (1998).
- [29] J. M. Caillol, J. Chem. Phys. **109**, 4885 (1998).
- [30] B. Smit, J. Chem. Phys. **96**, 8639 (1992).



## Tables

Tab. I: Sensitivity of free energy, pressure, and chemical potential at  $\rho^* = 1$  and  $\rho^* = 0.7$  to the choice of  $\sigma_{\text{H}}$ . For any quantity  $X$ ,  $\Delta X$  is the difference between the results obtained with  $a_{\text{BFC}} = 2.3$  and  $a_{\text{BFC}} = 2.5$ . The columns  $\Delta X/X$  and  $\Delta X/(dX/d\rho)$  relate the response of both the value and the slope of  $X$  as a function of  $\rho$  and so characterize the sensitivity of the shape of  $X(\rho)$  to variation of  $a_{\text{BFC}}$ . — In general, the free energy is seen to be far more forgiving than  $P$  and  $\mu$  with respect to the precise choice of  $\sigma_{\text{H}}$ , especially at low temperature.

## Figures

Fig. 1: Dependence of the BAS SCOZA excess free energy  $A^{\text{ex}}$  on the effective hard core diameter  $\sigma_{\text{H}}$  for the four states considered in Ref. [16]. (This corresponds to Fig. 2 of Ref. [16].)

Fig. 2: The pressure  $P$  as a function of  $\rho$  along four isotherms as computed within BAS SCOZA with the BFC diameters with  $a_{\text{BFC}} = 2.3, 2.5$  and  $e$ , as well as the simulation data of Ref. [25]. (This corresponds to Fig. 5 of Ref. [15].) The inset gives a detailed view of the isotherm at  $T^* = 1.4$ , along with the curves obtained in an MSA based variant of the theory ( $K = \beta$ ) for  $a_{\text{BFC}} = 2, 2.3$ , and  $e$ .

Fig. 3: The excess free energy  $A^{\text{ex}}$  as a function of  $\rho$  along four isotherms as computed with the BFC diameter with  $a_{\text{BFC}} = 2.3, 2.5$ , and  $e$ .

Fig. 4: Dependence of the chemical potential  $\mu$  on the effective hard core diameter  $\sigma_{\text{H}}$  for the four states considered in Ref. [16].

Fig. 5: The curve of phase coexistence as obtained for  $a_{\text{BFC}} = 2.2, 2.3, 2.5$ , and  $e$  as well as with the BH diameter, along with simulation results of Ref. [27]. All data refer to a truncated but not shifted, rather than the full, LJ potential.

Fig. 6: The curve of phase coexistence as obtained for  $a_{\text{BFC}} = 2.2, 2.3, 2.5$ , and  $e$  as well as with the BH diameter, along with simulation results of Ref. [26]. All data refer to the full LJ potential.

Fig. 7: SCOZA ( $A_{\text{HA}}^{\text{ex}}$ ) and BAS ( $\Delta A_{\text{S}}$ ) contributions to the BAS SCOZA excess free energy at  $T^* = 1.35$ ,  $\rho^* = 0.65$  for varying  $\sigma_{\text{H}}$ . Clearly, the SA free energy  $A^{\text{ex}} = A_{\text{HA}}^{\text{ex}} + \Delta A_{\text{S}}$  is far less sensitive to  $\sigma_{\text{H}}$  than either  $A_{\text{HA}}^{\text{ex}}$  or  $\Delta A_{\text{S}}$  taken by itself. On the other hand,  $A^{\text{ex}}$  is not quite constant as must be the case for an exact theory.

Fig. 8: Diameter dependence of the internal energy at four different states.

Fig. 9: SCOZA ( $U_{\text{HA}}^{\text{ex}}$ ) and BAS ( $\Delta U_{\text{S}}$ ) contributions to the BAS SCOZA internal energy at  $T^* = 1.35$ ,  $\rho^* = 0.65$  and  $T^* = 1.5$ ,  $\rho^* = 0.3$  for varying  $\sigma_{\text{H}}$ .

Fig. 10: BAS SCOZA and simulation [25] results for the configurational internal energy  $U^{\text{ex}}$  along four different isotherms for three choices of  $a_{\text{BFC}}$ . (This corresponds to one panel of Fig. 4 of Ref. [16].)

$\rho^*$	$T^*$	$\left  \frac{\Delta A^{\text{ex}}}{A^{\text{ex}}} \right $	$\left  \frac{\Delta A^{\text{ex}}}{dA^{\text{ex}}/d\rho^*} \right $	$\left  \frac{\Delta P}{P} \right $	$\left  \frac{\Delta P}{dP/d\rho^*} \right $	$\left  \frac{\Delta \mu}{\mu} \right $	$\left  \frac{\Delta \mu}{d\mu/d\rho^*} \right $
0.7	4.0	$2.6 \cdot 10^{-3}$	$7.8 \cdot 10^{-4}$	$8.0 \cdot 10^{-4}$	$2.0 \cdot 10^{-4}$	$9.5 \cdot 10^{-3}$	$1.7 \cdot 10^{-3}$
	2.5	$5.0 \cdot 10^{-3}$	$5.2 \cdot 10^{-4}$	$1.1 \cdot 10^{-3}$	$2.3 \cdot 10^{-4}$	$1.0 \cdot 10^{-2}$	$1.0 \cdot 10^{-3}$
	1.4	$8.5 \cdot 10^{-4}$	$2.5 \cdot 10^{-3}$	$1.2 \cdot 10^{-2}$	$1.4 \cdot 10^{-3}$	$2.6 \cdot 10^{-3}$	$3.1 \cdot 10^{-4}$
	0.75	$6.7 \cdot 10^{-4}$	$7.6 \cdot 10^{-4}$	$3.5 \cdot 10^{-2}$	$2.6 \cdot 10^{-2}$	$6.6 \cdot 10^{-3}$	$2.3 \cdot 10^{-2}$
1.0	4.0	$4.0 \cdot 10^{-4}$	$1.4 \cdot 10^{-4}$	$4.8 \cdot 10^{-3}$	$1.2 \cdot 10^{-3}$	$2.1 \cdot 10^{-3}$	$5.9 \cdot 10^{-4}$
	2.5	$3.2 \cdot 10^{-3}$	$7.1 \cdot 10^{-4}$	$1.0 \cdot 10^{-2}$	$2.2 \cdot 10^{-3}$	$8.3 \cdot 10^{-3}$	$1.9 \cdot 10^{-3}$
	1.4	$6.2 \cdot 10^{-2}$	$2.4 \cdot 10^{-3}$	$2.1 \cdot 10^{-2}$	$3.5 \cdot 10^{-3}$	$2.5 \cdot 10^{-2}$	$3.6 \cdot 10^{-3}$
	0.75	$8.0 \cdot 10^{-3}$	$6.2 \cdot 10^{-3}$	$4.4 \cdot 10^{-2}$	$4.6 \cdot 10^{-3}$	$2.4 \cdot 10^{-1}$	$5.0 \cdot 10^{-3}$

TABLE I:

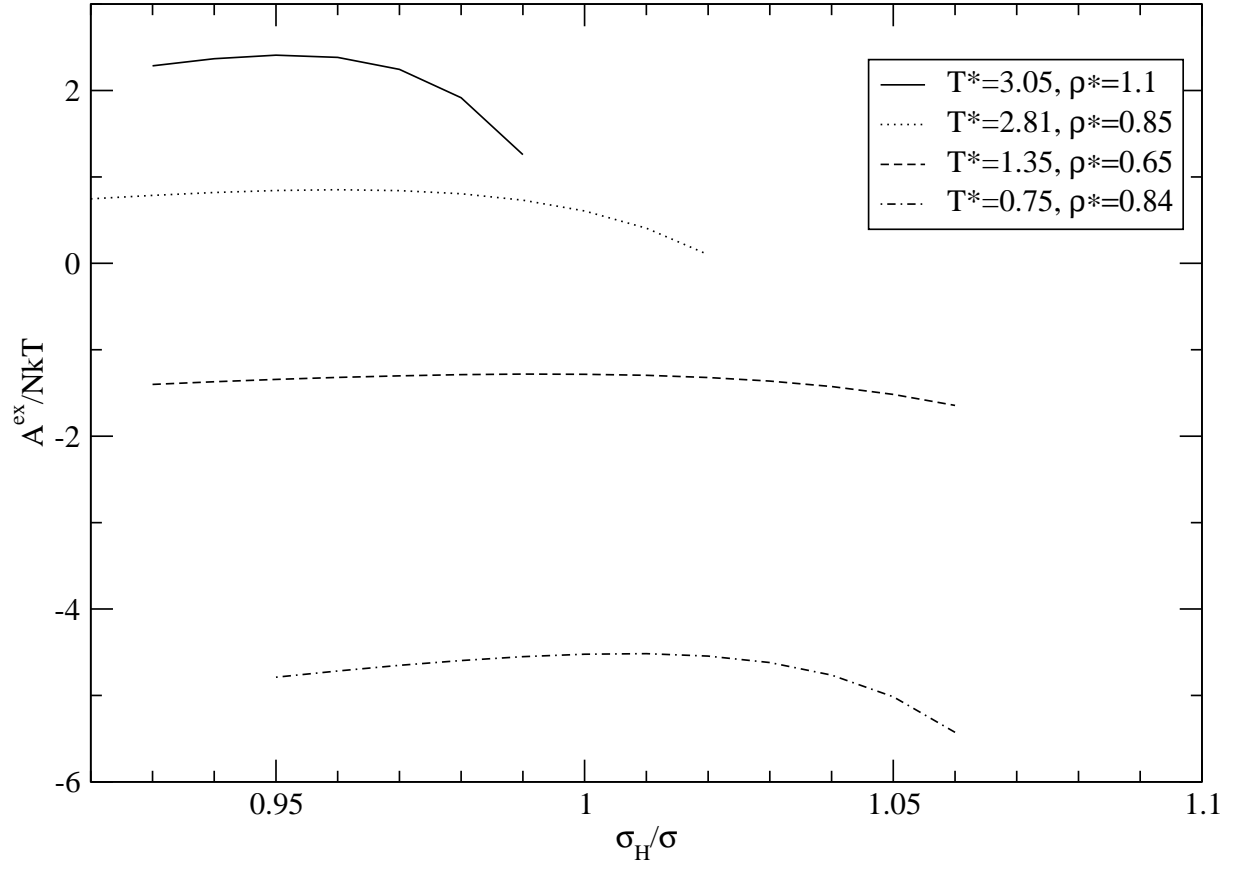


FIG. 1:

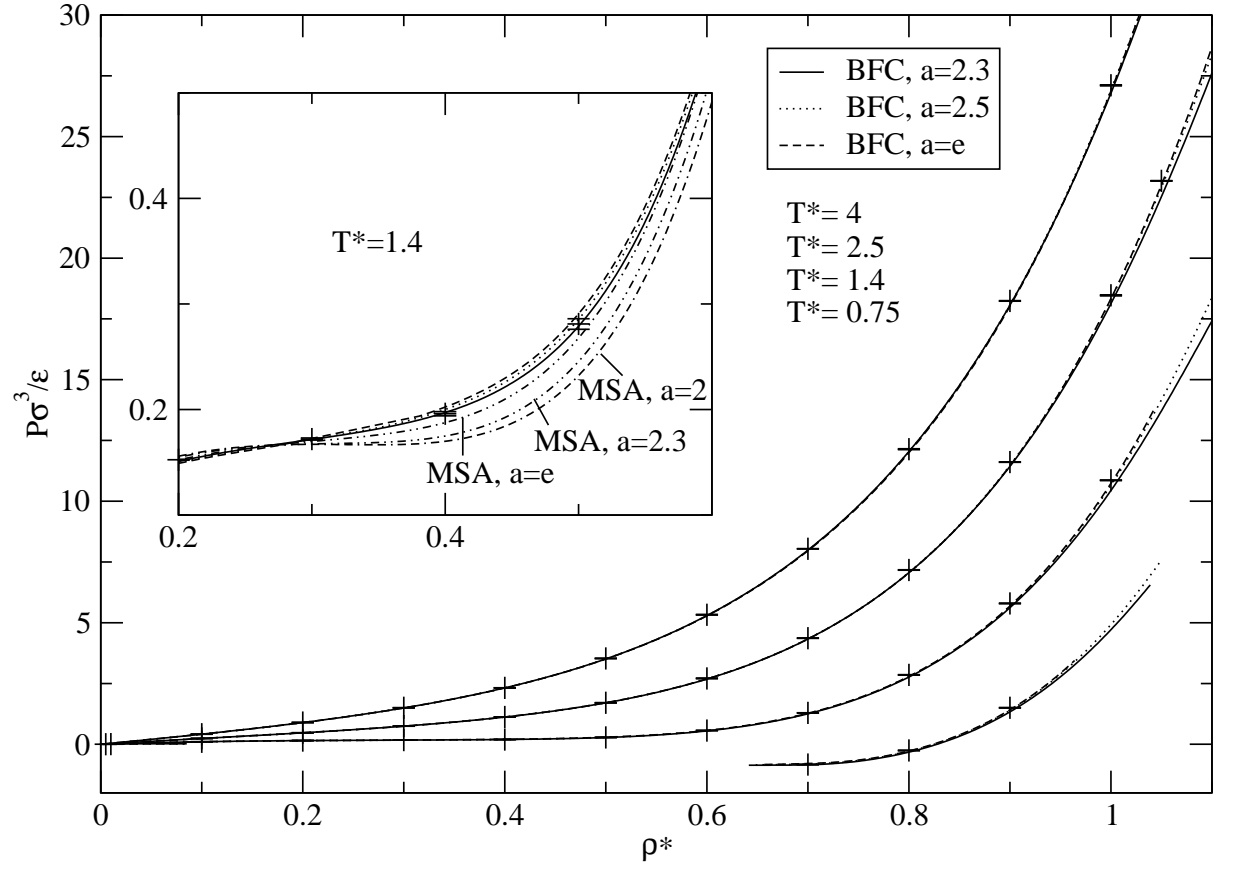


FIG. 2:

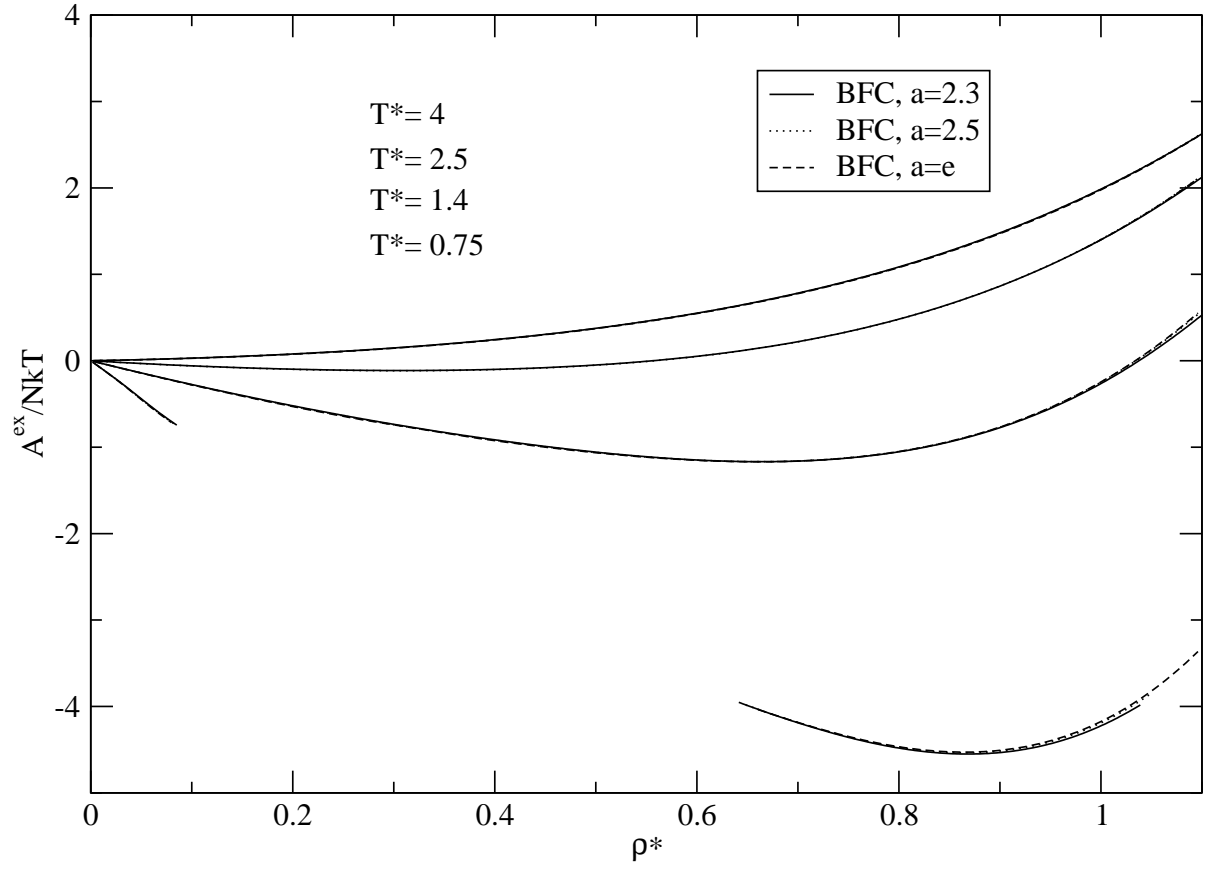


FIG. 3:

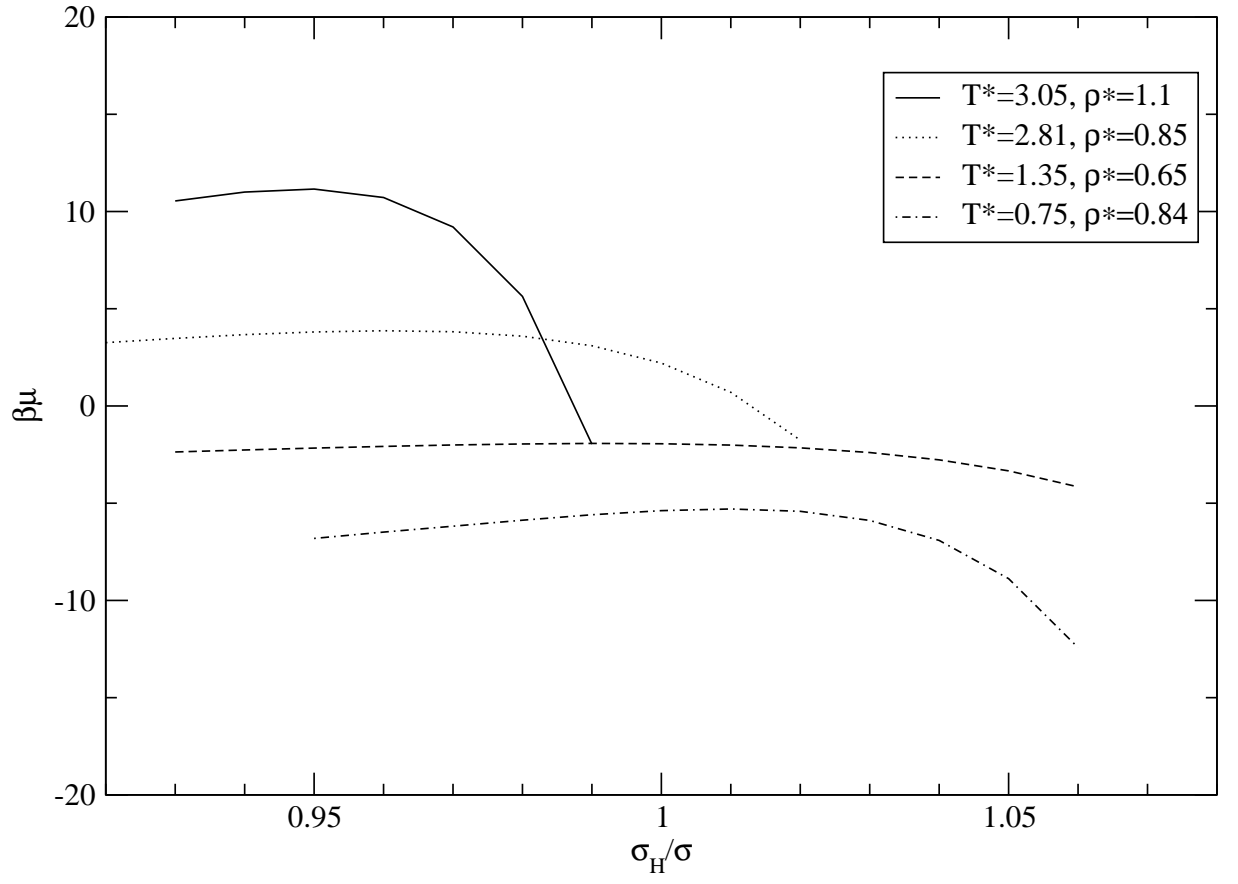


FIG. 4:



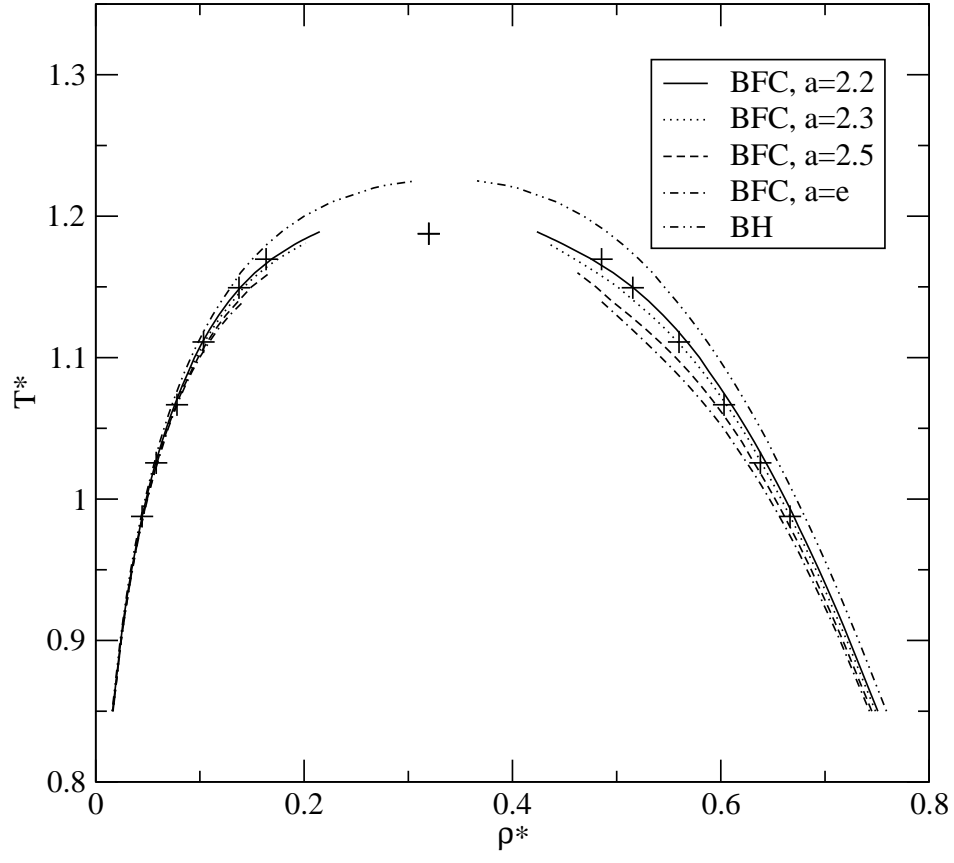


FIG. 5:

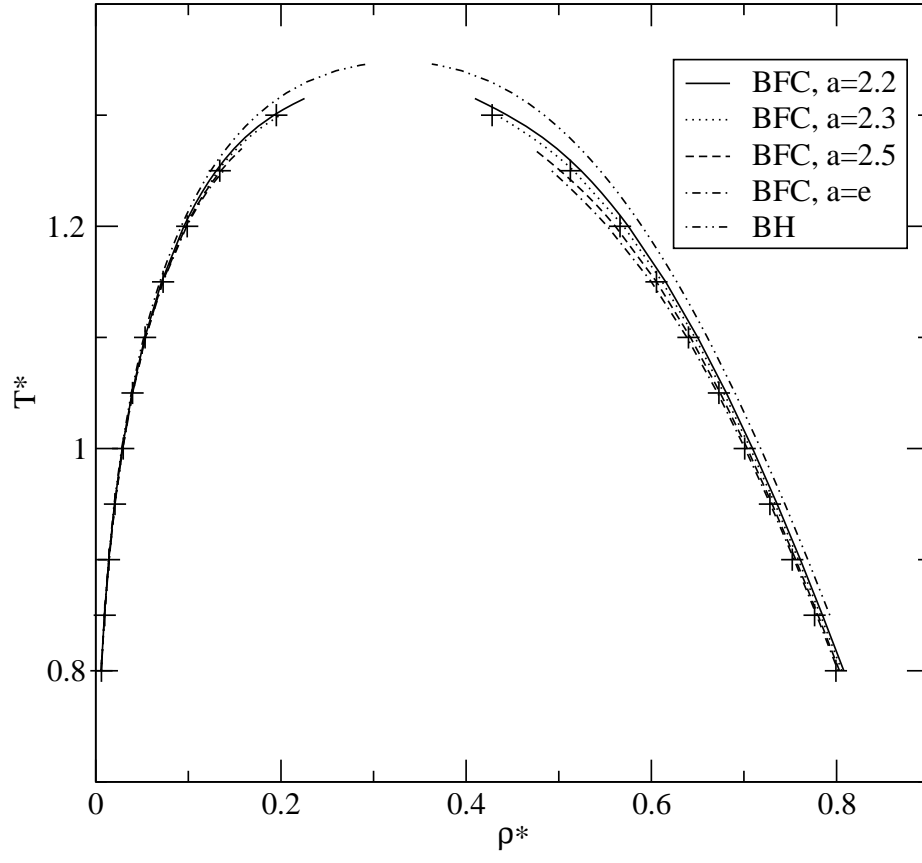


FIG. 6:

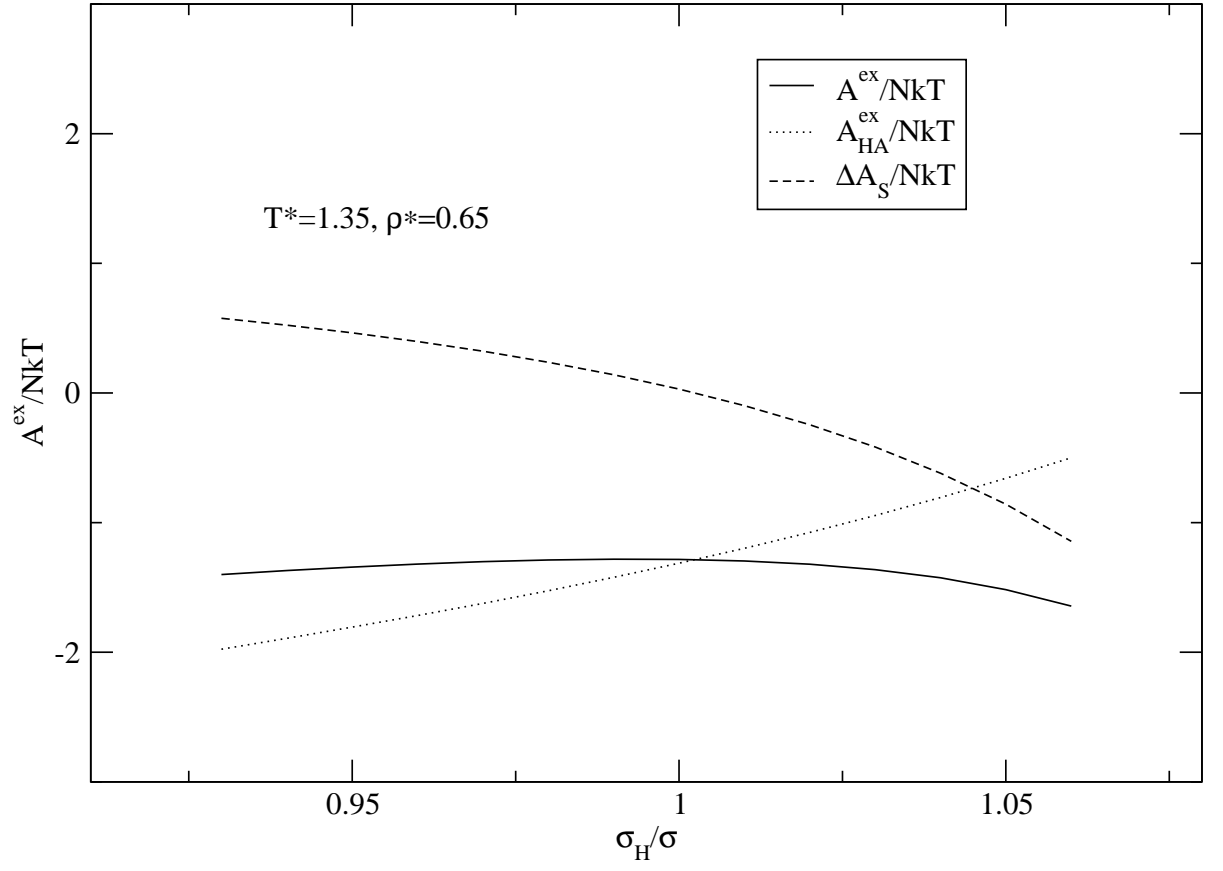


FIG. 7:

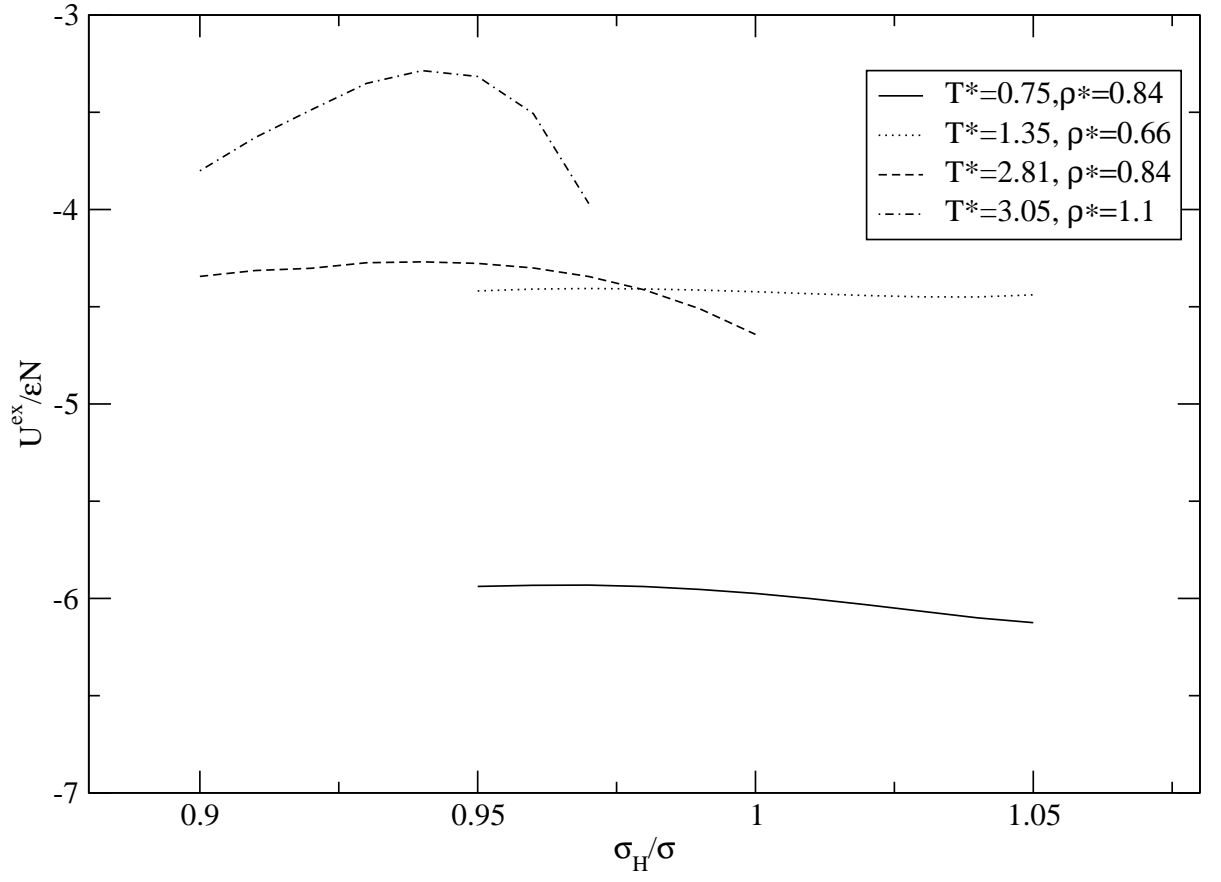


FIG. 8:

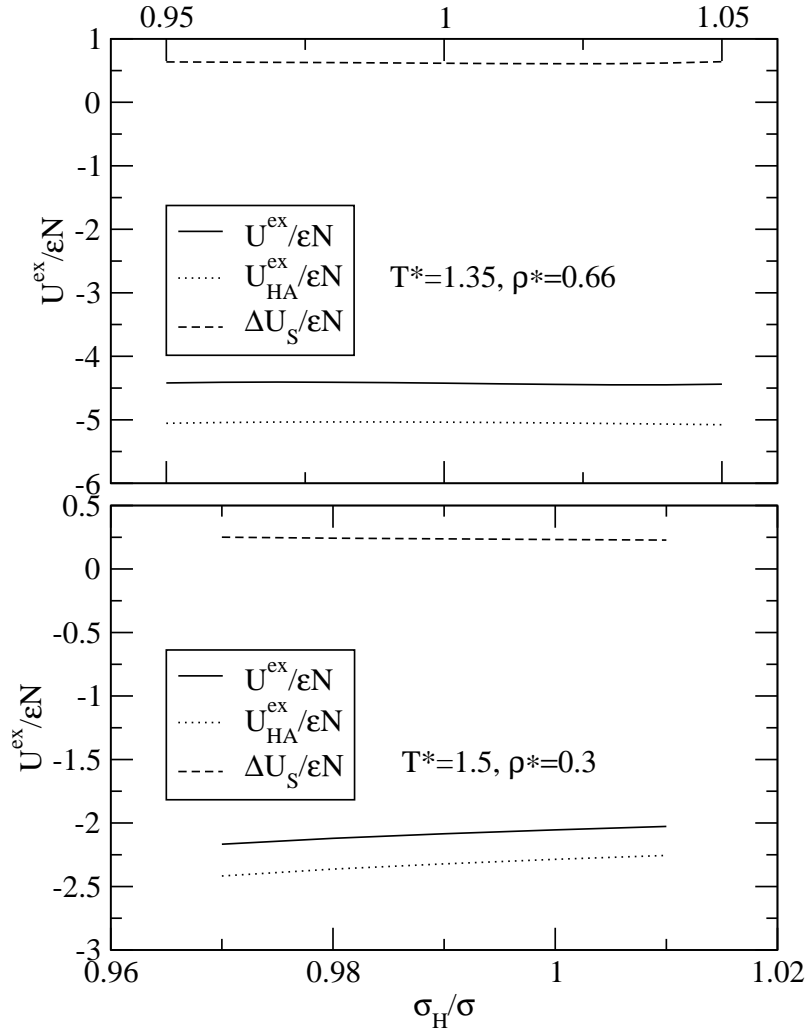


FIG. 9:

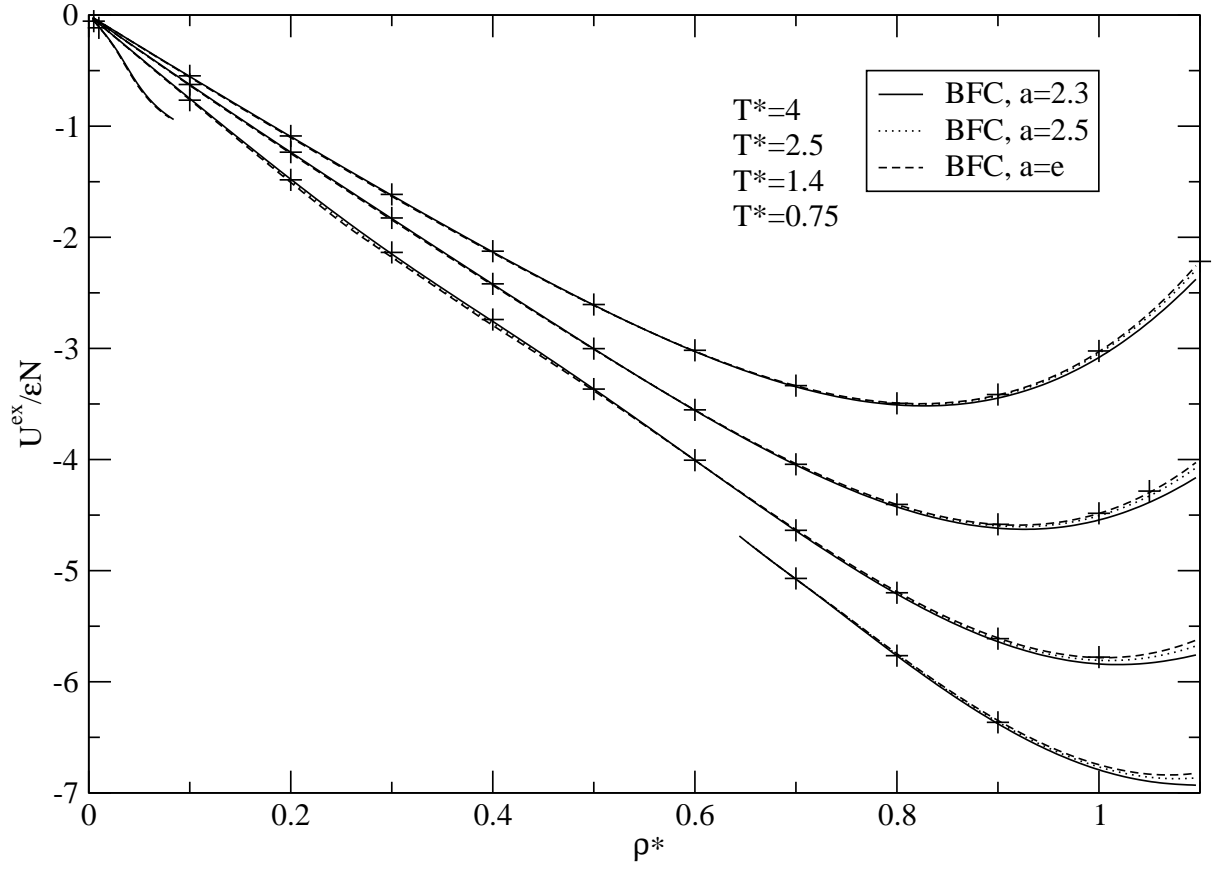


FIG. 10: